http://dx.doi.org/10.4322/2357-9730.73847

Imaging findings in Osteogenesis imperfecta

Matheus Dorigatti Soldatelli[1], Vanessa Döwich[1], Thaylla Maybe Bedinot da Conceição[1], Têmis Maria Félix[2]

Clin Biomed Res. 2017;37(3):266-268

1 Department of Radiology, Hospital de Clínicas de Porto Alegre (HCPA). Porto Alegre, RS, Brazil.

2 Department of Medical Genetics, Hospital de Clínicas de Porto Alegre (HCPA). Porto Alegre, RS, Brazil.

Corresponding author:
Matheus Dorigatti Soldatelli
md.soldatelli@gmail.com
Serviço de Radiologia, Hospital de Clínicas de Porto Alegre (HCPA)
Rua Ramiro Barcelos, 2350.
90035-903, Porto Alegre, RS, Brazil.

A 14-month-old male patient was brought to the outpatient clinic with a history of multiple bone fractures. He was born with fractures in the left femur and humerus and presented three more fractures before the first consultation. At physical examination, short stature, discolored teeth, triangular face shape, and bluish color of eye sclera were noticed. Initial radiographic studies of bones showed diffuse signs of osteoporosis, deformed limb bones, and multiple long bone fractures with different ages. The radiograph of the skull showed small intra-sutural bones lying between the cranial sutures, known as Wormian bones (Figure 1). Diagnosis of osteogenesis imperfecta (OI) was confirmed and treatment with cyclic sodium pamidronate was started. By the age of three, the patient sustained a total of 10 fractures. The bones involved were the left humerus, both femora and both tibiae. The following radiographic studies showed the "zebra stripe sign" – sclerotic growth recovery lines in the metaphysis of long bones (Figures 2 and 3).

OI is a rare, hereditary disorder of bones and connective tissues due to mutations affecting the synthesis of type I collagen and has an estimated prevalence of 6-7/100,000 births[1]. Individuals with OI have a lifelong risk of fracture, which may occur spontaneously or following minimal trauma. Other skeletal manifestations include short stature and progressive deformities of the skeleton. Systemic features are blue sclera, grayish/yellowish teeth (dentinogenesis imperfecta), early-onset hearing loss, basilar invagination, cardiovascular disease, and glaucoma[1-3].

The diagnosis of OI is typically made on the basis of personal and family medical history, physical examination, radiography and, in some cases, bone densitometry and DNA-based sequencing[2]. Despite having no pathognomonic features, conventional radiography still remains the mainstay in the diagnosis of OI. The most frequent findings are osteopenia (cortical bone thinning and trabecular bone rarefaction), long bone fractures, and skeletal deformities. Bone deformities occur most frequently in the appendicular skeleton and skull. In the long bones, bending and thinning of the diaphysis may be complicated by fractures in the concave aspect of the deformity, the typical shepherd's crook deformity of the femur (anterolateral bowing) and "saber shin" deformity of the tibia (anterior bowing) are described. In the skull, the most common findings are multiple Wormian bones embedded in the sutures[2,3].

The main differential diagnosis for OI is non-accidental injury (NAI) (child abuse). Although not easily distinguishable, some findings may suggest NAI, such as posterior rib fractures, metaphyseal corner fractures, complex skull fractures in the absence of signs of osteopenia, bone deformities, Wormian bones, and other systemic manifestations of OI[4].

There is no cure for OI and the treatment remains based on bisphosphonate therapy, orthopedic care, rehabilitation, and nutrition. On radiographs, specific findings in children receiving bisphosphonates include dense metaphyseal lines parallel to the growth plate (the so-called zebra stripe sign) that move towards the diaphysis along with bone growth. Each line corresponds to one intravenous course and the space between two lines depends on bone growth rate and the delay between two courses[1,3,5].

ISSN 2357-9730

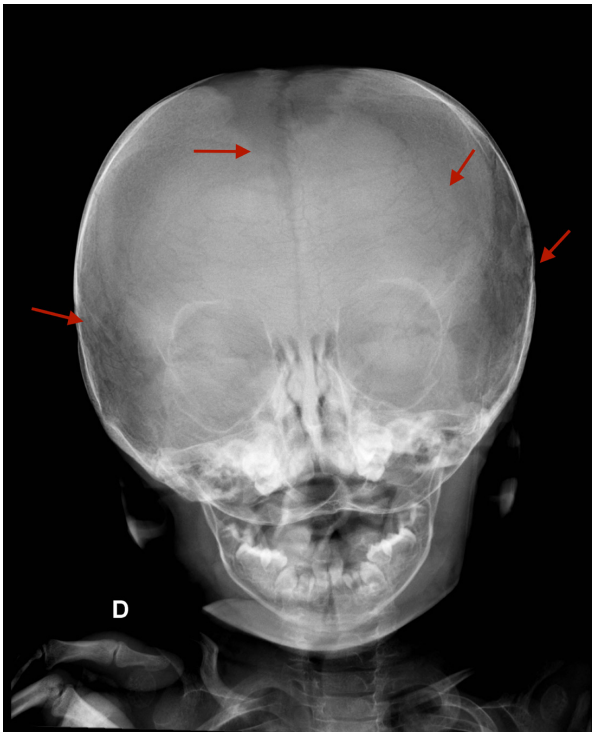

Figure 1: Anteroposterior radiograph of the skull (D: right side). Many small intra-sutural bones lying between the cranial sutures, known as Wormian bones, are seen (red arrows). Despite being a common finding in osteogenesis imperfecta, they are not specific of the disease.

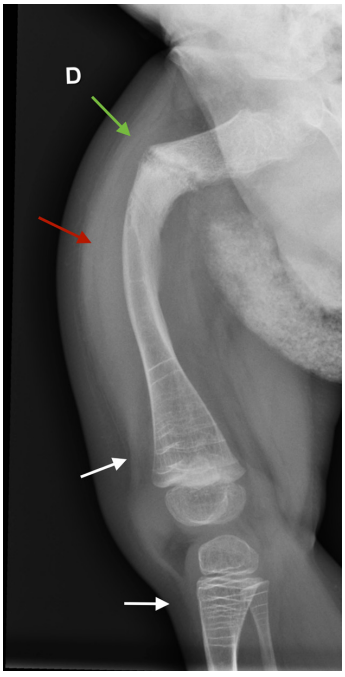

Figure 2: Anteroposterior radiograph of the thigh (D: right side). Signs of diffuse osteoporosis, anterolateral bowing deformity of the femur, known as shepherd´s crook (red arrow), and complete fracture of proximal femoral diaphysis (green arrow). The so-called zebra stripe sign from bisphosphonate therapy is also seen in long bones metaphysis (white arrows).

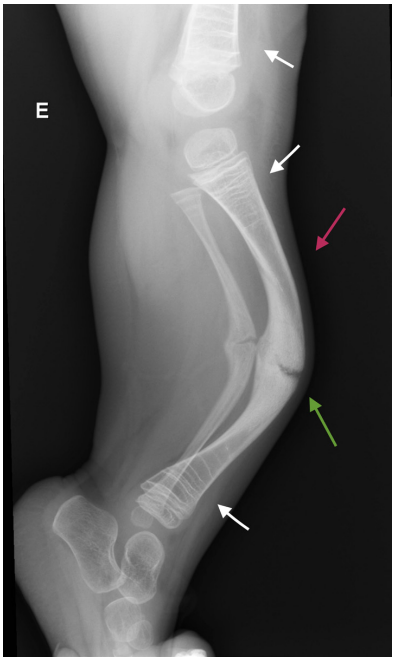

Figure 3: Lateral radiograph of the leg (E: left side). Signs of diffuse osteoporosis, anterior bowing deformity of the tibia, known as saber shin (pink arrow), and incomplete mid-diaphyseal fractures of the tibia and fibula are seen (green arrow). Also, the zebra stripe sign can be noticed in long bones metaphysis (white arrows).

REFERENCES

1. Brizola E, Félix TM, Shapiro JR. Pathophysiology and therapeutic options in osteogenesis imperfecta: an update. *Res Rep Endocr Disord*. 2016;6:17-30.

2. Renaud A, Aucourt J, Weill J, Bigot J, Dieux A, Devisme L, et al. Radiographic features of osteogenesis imperfecta. *Insights Imaging*. 2013;4(4):417-29. PMid:23686748. http://dx.doi.org/10.1007/s13244-013-0258-4.

3. Greenspan A. *Orthopedic imaging: a practical approach*. 5th ed. Philadelphia: Wolters Kluwer Lippincott Williams & Wilkins; 2010.

4. Kleinman PK. Differentiation of child abuse and osteogenesis imperfecta: medical and legal implications. *AJR Am J Roentgenol*. 1990;154(5):1047-8. PMid:2108540. http://dx.doi.org/10.2214/ajr.154.5.2108540.

5. Palomo T, Fassier F, Ouellet J, Sato A, Montpetit K, Glorieux FH, et al. Intravenous bisphosphonate therapy of young children with osteogenesis imperfecta: skeletal findings during follow up throughout the growing years. *J Bone Miner Res*. 2015;30(12):2150-7. PMid:26059976. http://dx.doi.org/10.1002/jbmr.2567.

Received: May 31, 2017
Accepted: Sep 02, 2017